Available online at www.sciencedirect.com
ScienceDirect
Dyes and Pigments 75 (2007) 11–24
DYES and PIGMENTS
www.elsevier.com/locate/dyepig

New thiophene-based azo ligands containing azo methine group in the main chain for the determination of copper(II) ions

Haluk Dinçalp [a,*], Fatih Toker [a], İnci Durucasu [a], Nesibe Avcıbaşı [b,c], Sıddık Icli [b,*]

[a] Department of Chemistry, Faculty of Art and Science, Celal Bayar University, Muradiye 45030 Manisa, Turkey
[b] Solar Energy Institute, Ege University, Bornova, 35100 Izmir, Turkey
[c] Ege Vocational Training School, Ege University, Bornova, 35100 Izmir, Turkey

Received 25 April 2006; accepted 8 May 2006
Available online 4 August 2006

Abstract

New kind of azo chromophores containing thiophene moiety and salicyaldimine-based ligand as side chains have been synthesized by a sequential process for optical sensing of Cu^{2+} metal ions in organic solution. Compounds have been characterized by IR and UV–vis spectrophotometer, ^{1}H NMR, ^{13}C NMR, MS, TGA and CV instruments. Spectral characteristics of the synthesized compounds have been investigated in five organic solvents of different polarity. Polarizibility effects of the solvents on the spectral characteristics and the dipole moments in the excited state are estimated. The fluorescence quantum yields of the synthesized compounds have been calculated to be in the range of 0.0035–0.0095 in solvents of different polarity. The fluorescence emission quenching experiments between the synthesized compounds and electron donor (pyrene, anthracene), electron acceptor (Co^{2+}) compounds give the bimolecular quenching rate constants of 10^{11} and 10^{14} M^{-1} s^{-1}, respectively. The free energies of photo-electron transfer process (ΔG_{ET}) between the azo dyes and the quenchers have been found to be about −19 kcal/mol. Cyclic voltammetry studies indicate that synthesized azo ligands undergo two- or three-reversible reduction potentials (versus ferrocene) and give LUMO energy value of −3.07 eV which is lower than that of TiO_2 conduction band and has a band gap value of ~2.5 eV. These results may point that synthesized azo dyes could be used as hole conducting materials in solid DSSC (Dye Sensitized Solar Cell) devices.

Thermal decomposition behavior of the azo dyes gives more information about the structure of the studied materials. The photoisomerization behavior of the synthesized compounds has been investigated in ethyl acetate under Xe lamp irradiation in the fluorescence spectrophotometer for 1 h. Photoisomerization rate constants of *cis–trans* orientation (k_{c-t}) have been found to be about 10^{-5} s^{-1}. The complexation process of synthesized thienylidene azo dyes gives subtle changes in their absorption spectra.

Keywords: Thienylidene azo dye; Azo methine; Solvatochromism; Photoisomerization; Stern–Volmer; Complex formation

1. Introduction

Azo compounds belong to one of the most intensively studied groups for non-linear optics (NLO) [1–3], optical information storage [4], and optical switching [5]. Besides their classical applications in synthetic dyes and pigments [6–8], they find increasing accessibility in photoresponsive biomaterials [9] and supramolecular systems [10]. They combine their optical and electronic properties with good chemical stability and solution processability [11,12], which makes them interesting for applications. Photochromism of azobenzene chromophores between *trans*-to-*cis* and *cis*-to-*trans* upon light irradiation is another remarkable property of azo compounds [13].

Azo ligands containing salicyaldimine-based ligand as side chains can be used in the production of chemical sensors because they show a significant change of color of the solution and maxima of the absorption band when they interact with

* Corresponding authors. Tel.: +90 232 3886025; fax: +90 232 3886027.
E-mail addresses: haluk.dincalp@bayar.edu.tr (H. Dinçalp), s_icli@yahoo.com, siddik.icli@ege.edu.tr (S. Icli).

0143-7208/$ - see front matter © 2006 Elsevier Ltd. All rights reserved.
doi:10.1016/j.dyepig.2006.05.015

transition metal ions. Transition metal-complexed azo methine compounds have been studied in great detail in the literature for understanding their optical and electronic properties, structure–redox relationships, mesogenic characteristics [14–17]. However, there are a limited number of studies in the literature which concern the combination of metal ions with azo ligands containing salicyaldimine-based ligand as side chains. Khandar and Nejati report the synthesis, characterization and cyclic voltammetry of Cu(II) complexes of a series of Schiff base ligands derived from condensation of 5-phenylazo salicylaldehyde with di- or tri-amines [18].

In this paper, versatile usable azo monomers combining with salicyaldimine-based ligand and nitro-substituted thiophene moiety have been designed and synthesized. Among the wide range of materials that may be suitable for the electronic and optical applications, salicyaldimine-based ligands are of particular interest. They find applications in preparation of metallomosegens [19], various crystallographic studies [14], optical metal ion detections [20], and enantioselective catalysis [21]. Also, salicylaldehyde gives more easily polymerization reaction of the 3- or 5-position of the structure. The Schiff bases derived from the reaction between oligosalicylaldehyde and amines are well-known in literatures [22,23]. Their excellent mechanical strength, good properties of stability, processability and functionalizability make them suitable for a number of applications in polymer industry [24–26]. Therefore, we plan to attach the thiophene moiety to the azo chromophores containing salicyaldimine-based ligand. The attachment of the nitro-substituted thiophene as side groups not only enables the extension of the conjugation length of the chromophore but also enhances the processability of the synthesized compound as NLO material in photoelectronic applications. Many researches report that thiophene derivatives have been widely used as conducting materials which are chemically more stable than other aromatic compounds [5,27,28]. These highly conjugated systems should exhibit very interesting electrochemical and redox behaviors because of the high electrically conducting property of thiophene moiety and good photochromic property of azo linkage. Also, salicyaldimine-based ligand as side chain should enhance the thermal stability of the compound.

Another aim of this study is to design push–pull chromophores which show good NLO (hyperpolarizability) activity. These kinds of chromophores consist of more extended conjugated system which contains strong electron donor, such as alkylamino-, and strong electron acceptor, such as nitro-groups in the main or side chains. Optical properties of NLO active materials are changed when the light passes through the material. Excited state charge-transfer efficiency of the chromophore plays an important role on the NLO activity. This efficiency is related to the more extended conjugation of the chromophore and strong polarizibility of the molecular structure.

Starting from the azo-coupling reaction between *p*-nitroaniline or 2-chloro-4-nitroaniline and *N*,*N*-dimethyl-*p*-phenylenediamine, we have synthesized 4-{3-[4-((*N*,*N*-dimethylaminophenyl)imino)methyl]-4-hydroxyphenylazo}-*N*-(5-nitro-2-thienylidene) aniline (**4a**) and 4-{3-[4-((*N*,*N*-dimethylaminophenyl)imino) methyl]-4-hydroxyphenylazo}-*N*-(5-nitro-2-thienylidene)-3-chloroaniline (**4b**) compounds. Molecular structures of the synthesized compounds are shown in Scheme 1. We have investigated the spectral characteristics of the synthesized compounds in solvents of different polarity. Also, electron donor/acceptor properties of the molecular structures have been explored by the quenching studies.

2. Experimental

2.1. Materials

All the chemical reagents and solvents used were purchased from Merck Chemical Company except 2-chloro-4-nitroaniline and chloroform. 2-Chloro-4-nitroaniline was supplied from Alfa Aesar. Chloroform was received from domestic chemical market and purified by distillation. Other chemical reagents were of analytical grade and used without further purification.

2.2. Instrumentation

The structures of the synthesized compounds were confirmed by ^{1}H and ^{13}C NMR spectra, recorded by a Bruker spectrometer operating at 400 MHz. FT-IR spectra were recorded on a Perkin–Elmer-Spectrum BX spectrophotometer in the region of 3000–400 cm^{-1} on KBr pellets. Melting points of all the compounds were determined on Electrothermal apparatus. Mass spectra of azo dyes **2a–b** were obtained with a DIP-mass technique on a Finnigan TSQ-700 (Thermoquest) spectrometer. Also, LC/MS analyses of thienylidene azo dyes **4a–b** were obtained on an Agilent 1100 MSD spectrometer. Thermal analyses were performed on a Perkin–Elmer Thermogravimetric Analyzer Pyris 6 TGA instrument under nitrogen atmosphere with 4.5 bar gas pressure. The samples were hold 1 min at initial temperature of 50 °C and, then heated to 700 °C for azo dyes **1a–b**, and to 1000 °C for the other dyes at a heating rate of 20 °C/min.

UV–vis spectra were obtained using a JASCO V-530 UV–vis spectrophotometer in the solutions. Complexation behavior of azo dyes **4a–b** with copper(II) ions was investigated using Specord S600-212C126 spectrophotometer. Fluorescence spectra were recorded on a PTI QM1 fluorescence spectrophotometer. Fluorescence quantum yields of the synthesized thienylidene azo dyes **4a–b** in organic solvents were calculated with reference to fluorescence emission of Rhodamine 6G ($\Phi_f = 0.95$ in ethanol, $\lambda_{exc} = 480$ nm) which was of spectrophotometric grade [29]. Also, all the compounds were analyzed at an optical density of below 0.1.

The spectroelectrochemical measurements of dyes were done on a CH instruments (Electrochemical Workstation) polarimeter. Cyclic voltammetry (CV) experiments of thienylidene azo dyes **4a–b** were carried out in a three-electrode cell consisting of a glassy carbon working electrode, a platinum counter electrode and Ag/AgCl (in saturated KCl solution) reference electrode. The redox potentials of the

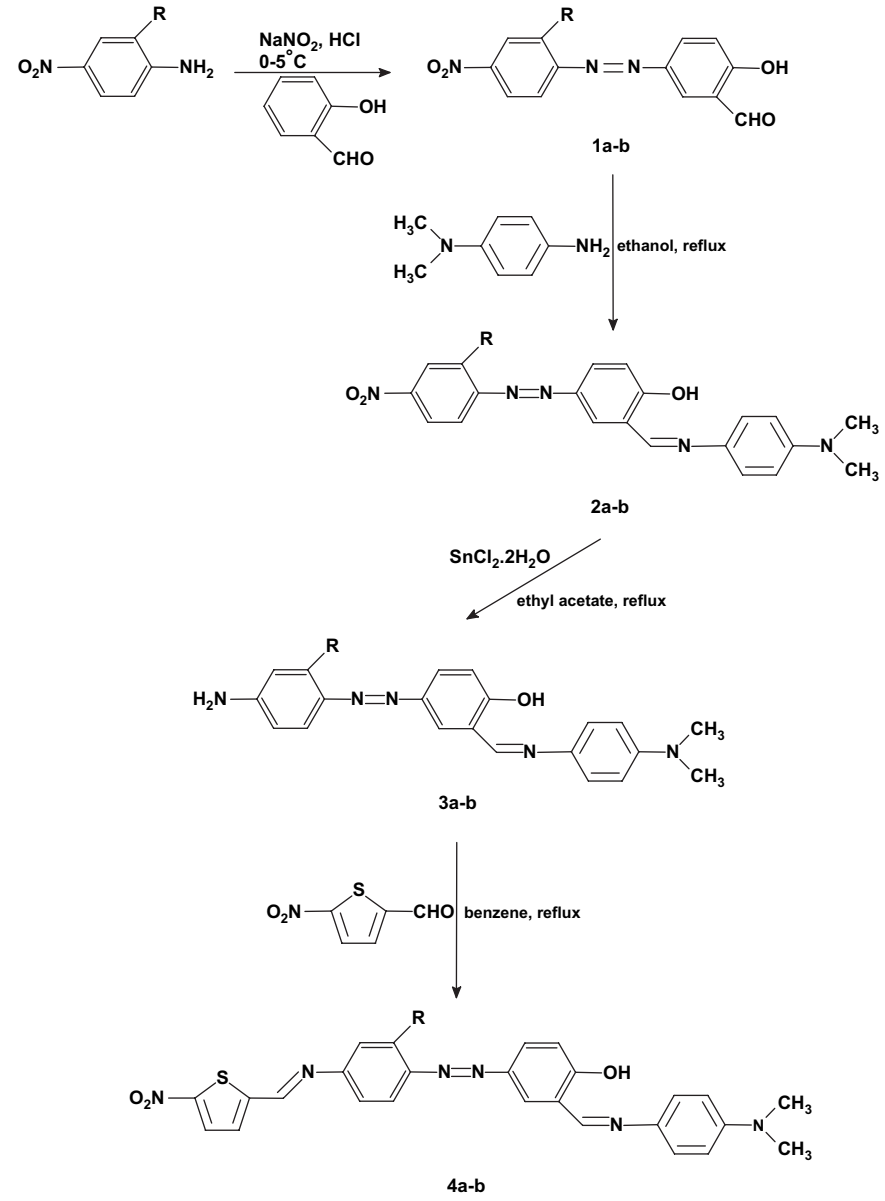

Scheme 1. Synthesis of thienylidene azo dyes **4a**–**b**.

compounds were controlled in the scale of −2/+2 V range. The supporting electrolyte was 100 mM [TBA][PF6] in acetonitrile. Millimolar solutions of the dyes were prepared in spectrophotometric grade acetonitrile. The oxidation potential of ferrocene which was used as an internal electrode was exhibited at about +0.45 V. Redox potentials of anthracene and pyrene used in quenching studies were taken as −1.09 V and −1.16 V versus calomel electrode [30]. Redox potential of Co^{2+} ion was obtained from the principles of instrumental analysis versus standard hydrogen electrode [31]. They were calculated by the formula $E_{cell} = E_{red} - E_{ox}$ with relative to Ag/AgCl electrode whose potential is at about 0.199 V versus NHE at 25 °C [32].

2.3. Synthesis

2.3.1. Synthesis of 1-(3-formyl-4-hydroxyphenylazo)-4-nitrobenzene (*1a*)

Azo dye **1a** was synthesized according to the well-known literature procedure [33]. A mixture of 5.52 g (40 mmol) of *p*-nitroaniline in 36 ml of hydrochloric acid, and 16 ml of water was heated to 70 °C to complete solution. The clear solution was poured into an ice–water mixture, and was diazotized between 0 °C and 5 °C with 2.8 g (40 mmol) of sodium nitrite dissolved in 10 ml of water. The cold diazo solution was added to the solution of 4.26 ml (40 mmol) of salicylaldehyde in 75 ml of water containing 1.6 g of sodium

hydroxide and 14.8 g of sodium carbonate during the period of 30 min at 0 °C. During the adding process, the diazo solution was vigorously stirred. The product was collected by filtration and washed with 100 ml of NaCl solution (10%) under vacuum. Then, the solid was dried under vacuum at 80 °C overnight. The purity of the compound was controlled by TLC (*n*-hexane:ethyl acetate/60:40).

$C_{13}H_9O_4N_3$, yield: 90%, m.p. = 185–186 °C. FT-IR (KBr, cm^{-1}): 3413 (–OH group), 3104, 1658 (–CHO group), 1606, 1524 and 1478 (–N=N–, *cis* and *trans*), 1342 (NO_2 group), 1284, 1173, 1103, 854, 768 cm^{-1}. UV–vis (toluene, nm): $\lambda_{max} = 360$ nm, $\varepsilon_{max} = 23\,900\ M^{-1}\,cm^{-1}$. ^1H NMR ($CDCl_3$, δ 7.26 ppm): $\delta = 11.43$ (1H, s); 10.05 (1H, s); 8.39 (2H, d); 8.27 (1H, t); 8.22 (1H, t); 8.01 (2H, d); 7.14 (1H, d) ppm.

2.3.2. Synthesis of 1-(3-formyl-4-hydroxyphenylazo)-2-chloro-4-nitrobenzene (*1b*)

2-Chloro-4-nitroaniline (7.9 g or 45 mmol) was used in the reaction. The same procedure and the same molar ratio of the reagents given in Section 2.3.1 were followed. The purity of the compound was controlled by TLC (*n*-hexane:ethyl acetate/60:40), and no extra purification was needed.

$C_{13}H_8O_4N_3Cl$, yield: 85%, m.p. = 127–128 °C. FT-IR (KBr, cm^{-1}): 3402 (–OH group), 3098, 1658 (–CHO group), 1525 and 1480 (–N=N–; *cis* and *trans*), 1343 (NO_2 group), 1287, 1191, 1102, 840, 750 cm^{-1}. UV–vis (toluene, nm): $\lambda_{max} = 373$ nm, $\varepsilon_{max} = 29\,670\ M^{-1}\,cm^{-1}$. ^1H NMR ($CDCl_3$, δ 7.25 ppm): $\delta = 11.50$ (1H, s); 10.05 (1H, s); 8.44 (1H, s); 8.30 (1H, s); 8.25 (1H, d); 8.21 (1H, d); 7.79 (1H, d); 7.17 (1H, d) ppm.

2.3.3. Synthesis of 1-{3-[4-((N,N-dimethylaminophenyl)-imino)methyl]-4-hydroxyphenylazo}-4-nitrobenzene (*2a*)

The title compound was prepared by a method reported in patent application [33]. A mixture of 3.0 g (11 mmol) of the azo dye **1a** and 1.5 g (11 mmol) of *N*,*N*-dimethyl-*p*-phenylenediamine in 30 ml of ethanol was refluxed under nitrogen atmosphere until the starting material could no longer be detected by TLC. It took time of 4 h. Then, the reaction mixture was vacuum filtered. The obtained product was purified by silica gel column chromatography with chloroform alone as eluent. The title compound was dried under vacuum at 70 °C overnight.

$C_{21}H_{19}O_3N_5$, yield: 77%, m.p. = 231–233 °C. FT-IR (KBr, cm^{-1}): 2909, 1620 (–CH=N– group), 1519 (–N=N– group), 1341 (NO_2 group), 1145, 1103, 855, 804 cm^{-1}. UV–vis (toluene, nm): $\lambda_{max} = 368$ nm, $\varepsilon_{max} = 26\,460\ M^{-1}\,cm^{-1}$. ^1H NMR ($CDCl_3$, δ 7.25 ppm): $\delta = 10.05$ (1H, s); 8.72 (1H, s); 8.37 (2H, dd); 8.27 (1H, s); 8.22 (1H, d); 8.02 (2H, dd); 7.30 (1H, d); 7.14 (2H, dd); 6.74 (2H, d); 3.06 (6H, s) ppm. DIP-mass: $[M]^{\bullet+} = 389$ molecular ion peak; 359 $[M]^{\bullet+} - 2CH_3$; 345 $[M]^{\bullet+} - N(CH_3)_2$; 271 $[M]^{\bullet+} - Ph-N(CH_3)_2$; 239 $[M]^{\bullet+} - N_2-Ph-NO_2$; 195 $[M]^{\bullet+} - N_2-Ph-NO_2-N(CH_3)_2$; 120 $[M-1]$ peak of $Ph-N(CH_3)_2$; 120 $[M-2]$ peak of Ph–OH; 77 $[M-1]$ peak of Ph–H.

2.3.4. Synthesis of 1-{3-[4-((N,N-dimethylaminophenyl)-imino)methyl]-4-hydroxyphenylazo}-2-chloro-4-nitrobenzene (*2b*)

The similar procedure given in Section 2.3.3 was followed. A mixture of 3.0 g (9.8 mmol) of the azo dye **1b** and 1.37 g (9.8 mmol) of *N*,*N*-dimethyl-*p*-phenylenediamine in (30 ml THF/18 ml ethanol) solvent system was heated to 75 °C under nitrogen atmosphere for 5 h and 30 min. The reaction was monitored by TLC method. Purification by column chromatography with chloroform:*n*-hexane/70:30 gave the azo dye **2b**.

$C_{21}H_{18}O_3N_5Cl$, yield: 73%, m.p. = 237–238 °C. FT-IR (KBr, cm^{-1}): 2804, 1616 (–CH=N– group), 1521 (–N=N– group), 1340 (NO_2 group), 1233, 1166, 1102, 889, 815 cm^{-1}. UV–vis (toluene, nm): $\lambda_{max} = 398$ nm, $\varepsilon_{max} = 23\,300\ M^{-1}\,cm^{-1}$. ^1H NMR ($CDCl_3$, δ 7.25 ppm): $\delta = 10.06$ (1H, s); 8.73 (1H, s); 8.44 (1H, d); 8.30–8.10 (2H, overlapped); 8.09 (1H, s); 8.07(1H, s); 7.80 (1H, d); 7.35 (2H, d); 7.16 (2H, d); 3.07 (6H, s) ppm. DIP-mass: $[M]^{\bullet+} = 423$ molecular ion peak (Cl-35 isotopes) and $[M]^{\bullet+} = 425$ molecular ion peak (Cl-37 isotopes); 393 $[M]^{\bullet+} - 2CH_3$; 359 $[M]^{\bullet+} - 2CH_3 - Cl$; 345 $[M]^{\bullet+} - N(CH_3)_2 - Cl$; 239 $[M]^{\bullet+} - N_2-PhCl-NO_2$; 195 $[M]^{\bullet+} - N_2-Ph(Cl)-NO_2-N(CH_3)_2$; 119 $[M-2]$ peak of $Ph-N(CH_3)_2$; 77 $[M-1]$ peak of Ph–H.

2.3.5. Synthesis of 4-{3-[4-((N,N-dimethylaminophenyl)-imino)methyl]-4-hydroxyphenylazo}aniline (*3a*)

Title compound was prepared using a procedure given in literature [34]. A mixture of 1 g (2.56 mmol) azo dye **2a**, 3 g (13.2 mmol) of $SnCl_2 \cdot 2H_2O$, and 0.004 g (0.036 mmol) of hydroquinone in 40 ml of ethyl acetate was heated to 77 °C under nitrogen atmosphere until no starting material could be detected on TLC plate. This was required for about 1 h and 30 min. The reaction was cooled down to room temperature and then added to ice–water mixture. The pH of the solution was adjusted to basic pH 8 by adding 50 ml of aqueous $NaHCO_3$ (10%) solution before being extracted with ethyl acetate. Organic phase was dried over sodium sulphate. After evaporation of the solvent, the crude product was purified by a silica gel chromatography column with chloroform:methanol (90:10) solvent system. Pure derivative **3a** would decompose slowly if it has been stored for a long time.

$C_{21}H_{21}ON_5$, yield: 70%. FT-IR (KBr, cm^{-1}): 3374 ($-NH_2$ group), 1629 (–CH=N– group), 1516 (–N=N– group), 1263, 1128, 824, 720 cm^{-1}.

2.3.6. Synthesis of 4-{3-[4-((N,N-dimethylaminophenyl)-imino)methyl]-4-hydroxyphenylazo}-3-chloroaniline (*3b*)

The same procedure given in Section 2.3.5 was followed. Purification was accomplished by column chromatography on silica with *n*-hexane/ethyl acetate (70:30) as eluent. Also, this compound showed decomposition activity under atmospheric conditions.

$C_{21}H_{20}ON_5Cl$, yield: 73%. FT-IR (KBr, cm^{-1}): 3337 (−NH_2 group), 2926, 1602 (−CH═N− group), 1505 (−N═N− group), 1303, 1236, 1153, 1040, 862, 818, 745 cm^{-1}.

2.3.7. Synthesis of 4-{3-[4-((N,N-dimethylaminophenyl)-imine)methyl]-4-hydroxyphenylazo}-N-(5-nitro-2-thienylidene)aniline (**4a**)

Freshly synthesized amino azo dye **3a** (0.3 g or 0.83 mmol) was dissolved in 44 ml of benzene under vigorous stirring. 5-Nitro-2-thiophenecarboxaldehyde (0.13 g or 0.83 mmol) was added to the solution under nitrogen atmosphere. The reaction temperature was controlled at 80 °C, and thus the reaction was completed for 1 h. The reaction mixture was vacuum filtered to give a red product which was then purified by a silica gel chromatography column with *n*-hexane:ethyl acetate (50:50) as an eluent.

$C_{26}H_{22}O_3N_6S$, yield: 85%, m.p. = 120−121 °C. FT-IR (KBr, cm^{-1}): 3361 (−OH group), 2924, 1616 (−CH═N− group), 1597 (−CH═N− group), 1493 (−N═N− group), 1438, 1329 (NO_2 group), 1111, 811, 731 cm^{-1}. ^{1}H NMR ($CDCl_3$, δ 7.21 ppm): δ = 9.90 (1H, s); 8.62 (1H, s); 8.47 (1H, s); 7.89 (1H, d); 7.83 (2H, d); 7.80 (1H, d); 7.62 (1H, d); 7.31 (2H, overlapped); 7.24 (2H, d); 7.17 (2H, d); 6.63 (2H, d); 2.96 (6H, s) ppm. ^{13}C NMR [$CDCl_3$ δ 77 ppm (3 peaks)]: 112−156 (20 different C-atoms including aromatic and imine C-atoms), 40.61 ($N(CH_3)_2$) ppm. LC/MS-APCI: $[M]^{\bullet+}$ = 498 molecular ion peak is not observed, but 387 $[M]^{\bullet+} - NO_2-OH-N(CH_3)_2$; 311 $[M]^{\bullet+} - NO_2-OH-Ph-N(CH_3)_2$; 276 $[M]^{\bullet+} - C_5H_3N_2O_2S-OH-N(CH_3)_2$; 262; 139; 122.

2.3.8. Synthesis of 4-{3-[4-((N,N-dimethylaminophenyl)-imino)methyl]-4-hydroxyphenylazo}-N-(5-nitro-2-thienylidene)-3-chloroaniline (**4b**)

The synthetic procedure given in Section 2.3.7 was used. Freshly synthesized amino azo dye **3b** (0.25 g or 0.63 mmol) and 5-nitro-2-thiophenecarboxaldehyde (0.10 g or 0.63 mmol) were heated to 80 °C under nitrogen atmosphere for 1 h. The reaction mixture was vacuum filtered and, then the solid was passed through a silica column (*n*-hexane:ethyl acetate/50:50). The title compound was dried under vacuum at 70 °C overnight.

$C_{26}H_{21}O_3N_6SCl$, yield: 78%, m.p. = 190−191 °C. FT-IR (KBr, cm^{-1}): 2901, 1608 (−CH═N− group), 1563 (−CH═N− group), 1527, 1493 (−N═N− group), 1426, 1365, 1328 (NO_2 group), 1222, 1034, 808, 730 cm^{-1}. ^{1}H NMR ($CDCl_3$, δ 7.25 ppm): δ = 9.96 (1H, s); 8.55 (1H, s); 8.20 (1H, s); 8.00 (1H, dd); 7.89 (1H, d); 7.87 (1H, d); 7.71(1H, d); 7.69 (1H, d); 7.52 (1H, dd); 7.33 (2H, overlapped); 6.75 (2H, d); 7.26 (2H, d); 3.03 (6H, s) ppm. ^{13}C NMR [$CDCl_3$ δ 77 ppm (3 peaks)]: 113−167 (22 different C atoms including aromatic and imine C atoms), 41.10 ($N(CH_3)_2$) ppm. LC/MS-APCI: $[M]^{\bullet+}$ = 532 molecular ion peak is not observed, but [M − 3] = 529 (Cl-35 isotopes) and [M − 3] = 531 (Cl-37 isotopes); 391 and 393 $[M]^{\bullet+} - C_5H_3NO_2S$; 343 $[M]^{\bullet+} - C_5H_3N_2O_2S-Cl$; 276 $[M]^{\bullet+} - C_5H_3N_2O_2S-Cl-OH-N(CH_3)_2$; 262; 167; 149; 151.

3. Results and discussion

3.1. Steady-state measurements and fluorescence quantum yield determination studies at room temperature

Fig. 1 shows the normalized UV−vis absorption spectra of azo dyes **1a** and **2a**, and thienylidene azo dye **4a** in toluene. The absorption maximum of azo dye **1a** is recognized at 360 nm arising from the π−π* transition in the backbone. The absorption spectrum of azo dye **2a** containing salicyaldimine-based ligand gives a red shift of 8 nm with respect to the same spectrum of azo dye **1a**. After attaching the nitro-substituted thiophene group as side chain, a significant red shift from 368 nm to 487 nm is observed for thienylidene azo dye **4a** in toluene because of the increasing of conjugation length in chromophore. Also, electronic effects of the nitro substituent on the thiophene ring change the absorption peak position of thienylidene azo dye **4a**. When introducing the chloride atom in the benzene ring, the absorption spectrum gives a marked red shift of 13 nm in toluene compared to the corresponding spectrum of azo dye **1a**. The absorption maximum of thienylidene azo dye **4b** is assigned at 490 nm in toluene from the n−π* transition in the visible region. The fluorescence spectra show emission maxima at 537 nm and 577 nm for thienylidene azo dye **4a**, and at 536 nm and 575 nm for thienylidene azo dye **4b** in toluene.

The tautomeric behaviors of thienylidene azo dyes **4a**−**b** have been examined by means of absorption, emission and excitation spectra in toluene at room temperature (Fig. 2). It is well-known that many salicylidene anilines exhibit intramolecular proton transfer reactions, and therefore attract considerable attention from experimental points of view [35−38]. Guha et al. have studied ground and excited state inter- and intramolecular proton transfer reactions of 7-ethylsalicylidene-benzylamine (ESBA) in different protic solvents and found that ESBA exhibits more than one structural form in the ground and excited states [35]. The main emission peak of compound **4a** occurs at a wavelength shorter than the minor

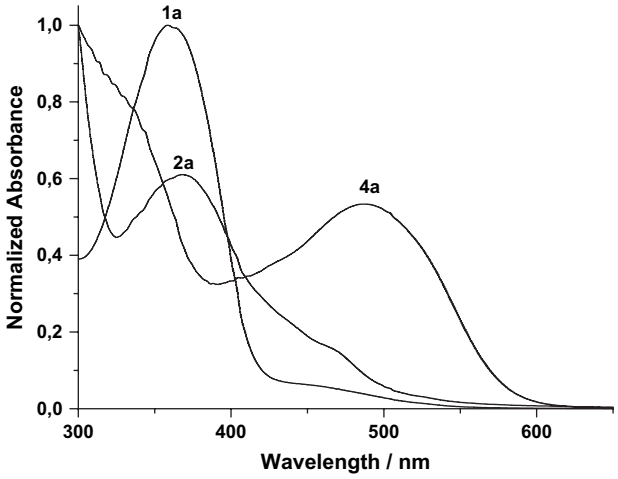

Fig. 1. Normalized UV−vis absorption spectra of azo dyes **1a** and **2a**, and thienylidene azo dye **4a** in toluene.

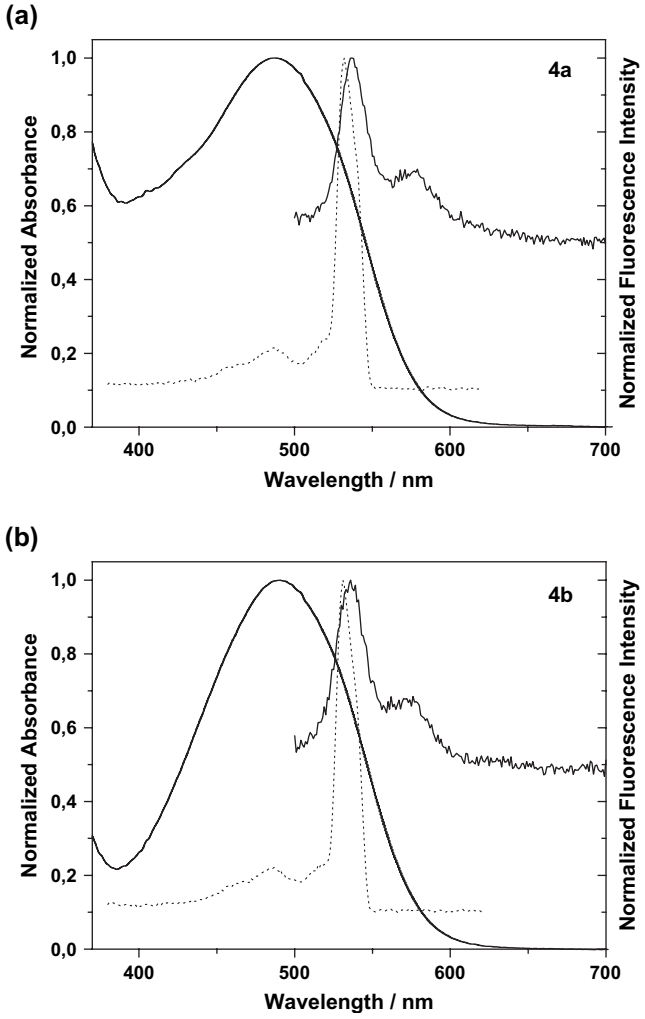

Fig. 2. Normalized visible absorption, emission and excitation (dotted line) spectra of (a) thienylidene azo dye **4a**, and (b) thienylidene azo dye **4b** in toluene at room temperature ($\lambda_{exc} = 480$ nm, $\lambda_{em} = 540$ nm).

peak, and the minor peak appears as a red-shifted shoulder on the main emission peak. No mirror image relationship is observed between the emission spectra and the ground state absorption spectra of the compounds **4a**–**b**. These extraordinary emission spectra may be attributed to formation of different excited state structure of the studied compounds. The excitation spectrum of compound **4a** at emission wavelength of 540 nm in toluene gives one sharp peak at 531 nm, and one broad peak at 487 nm. The excitation spectrum is not identical with the absorption spectra of compound **4a**. The non-mirror image relationship between the emission and absorption spectra, and the shape of the excitation spectra give a subtle explanation of excited state intramolecular proton transfer reaction. In this reaction, excited enol form of the compound is converted to the keto form as shown in Scheme 2. Emission spectrum belongs to the keto form of compound **4a**. Also, large Stokes shift supports the occurrence of fast proton transfer reaction in the excited state. The emission and excitation measurements have been repeated in more polar chloroform solution and the same tautomeric behaviors of the compounds **4a**–**b** have been obtained (data not shown). These results are

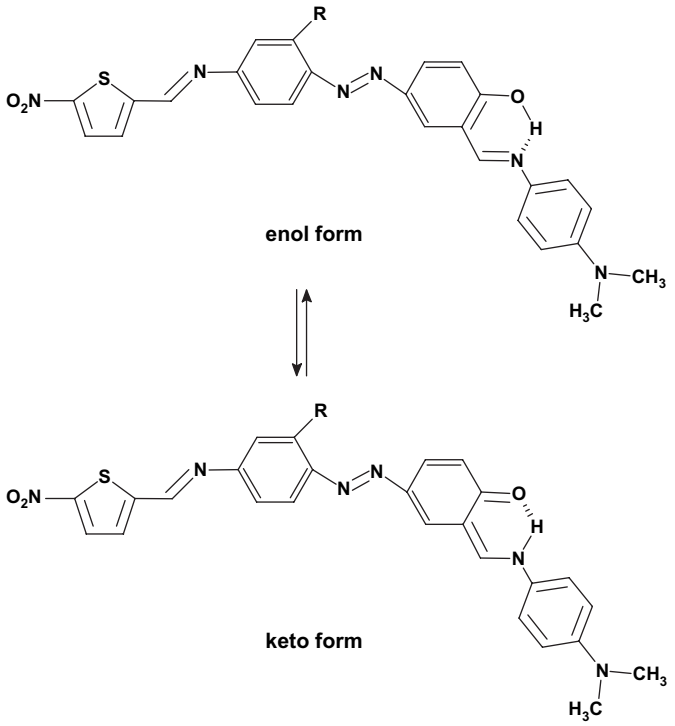

Scheme 2. Possible structural configurations of thienylidene azo dyes **4a**–**b**.

in agreement with the literature data. Alarcón et al. have studied the tautomeric behavior of a series 2-hydroxybenzaldehydes and found that emission comes only from the keto form of the studied compounds [39].

Spectral characteristics of thienylidene azo dyes **4a**–**b** in increasing solvents of polarity have been examined as shown in Fig. 3 and also summarized in Table 1. In general, it is seen that higher the dielectric constants of the solvents, the more increase the red-shifted wavelength of absorption maxima of the compounds, excluding in chloroform solution. This may be attributed to the hyperpolarizability activity of the studied compounds in the excited states. The more polar form is observed in the excited state with respect to the ground state when the molecule is excited. Increasing solvent polarity reduces the LUMO energy level of the studied compounds with a higher ratio relative to the HOMO energy level so that a bathochromic shift is observed in polar solvents with respect to the less polar solvents. In chloroform, a strange increase is observed at the absorption maxima of the compounds. Hydrogen bonding ability of the chloroform with the studied molecules facilitates the formation of intermolecular hydrogen bonded enolic form and stabilizes the charge-transfer excited state. Therefore, absorption spectrum is seen to shift to long-wavelength region. These results are in well accordance with the literature data. It is well-known that this red shift maximum in more polar media is due to the formation of intermolecular hydrogen bonded complex with the solvent molecules [35–39].

Comparison of fluorescence quantum yields of thienylidene azo dyes **4a**–**b** in solvents of different polarity are shown in Fig. 4 and, also summarized in Table 2. It is clearly seen

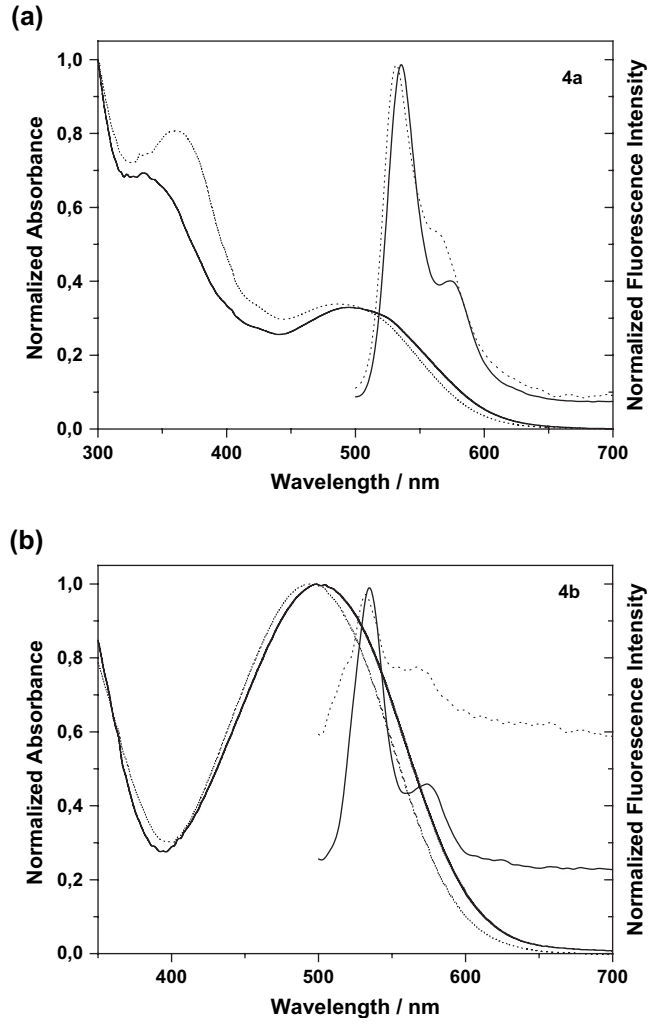

Fig. 3. Normalized visible absorption and fluorescence spectra of (a) thienylidene azo dye **4a**, and (b) thienylidene azo dye **4b** in chloroform (solid line) and tetrahydrofuran (dotted line) solutions ($\lambda_{exc} = 480$ nm).

that both the compounds have very small quantum yield values in all of the studied solvents. As a general rule, azo dyes do not fluoresce [9]. Also, the low quantum yields can be explained by the increase in non-radiative relaxation process [41].

Table 1
The visible absorptions, fluorescence emissions, and Stokes shifts ($\Delta\lambda$) data of thienylidene azo dyes **4a–b** in solvents of different polarity (λ/nm, ε/$1\,mol^{-1}\,cm^{-1}$) ($\lambda_{exc} = 480$ nm)

Solvent	ε[a]	Compound	λ_1	ε_1	$\lambda_{em\ (max)}$	$\Delta\lambda$
Toluene	2.4	**4a**	487	2150	537	57
		4b	490	11 420	536	56
Chloroform	4.8	**4a**	496	1880	536	56
		4b	500	7600	534	54
Ethyl acetate	6.0	**4a**	480	1680	528	48
		4b	486	6060	527	47
Tetrahydrofuran	7.6	**4a**	487	1610	532	52
		4b	495	4640	533	53
Dichloromethane	8.9	**4a**	502	1580	535	55
		4b	505	4292	531	51

[a] Dielectric constant, ε, is taken from Ref. [40].

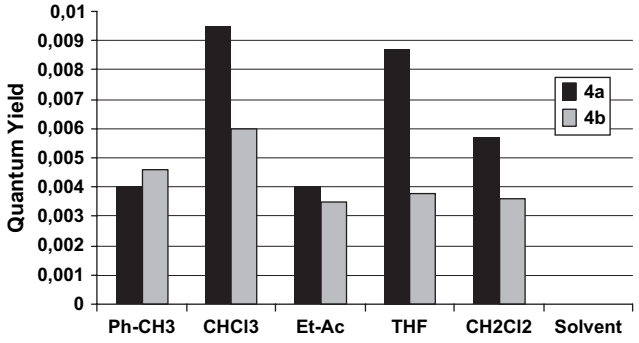

Fig. 4. Comparison of fluorescence quantum yields of thienylidene azo dyes **4a–b** in 5 solvents of increasing polarity.

Another reason explaining the low quantum yield is the high aggregation tendency of the molecules caused by the presence of nitro group in the structure [9]. The highest quantum yields have been calculated in chloroform solution for both the compounds. This behavior may be attributed to the formation of intermolecular hydrogen bonded enolic form of the studied compounds in more polar chloroform solution. This conformer favors the formation of tautomeric structure of the compound so that the more planar structural form of thienylidene azo dye **4** is obtained. Rotation about the azo linkages is inhibited. Therefore, conformational relaxation is reduced in chloroform with respect to the other studied solutions.

It is clearly seen that fluorescence quantum yields of compound **4b** are lower than the corresponding yields for compound **4a** in the studied solvents. Because heavy atom isotope affect of the chloride atom in compound **4b** decreases the electronic cloud intensity. This reduction in electronic cloud causes the decreasing of fluorescence quantum yields.

We cannot detect the fluorescence decay times of the compounds with single photon counting method because of both very low emission signals and short fluorescence decay time values at room temperature. Fluorescence lifetimes are estimated from $\tau_f = \tau_0 \times \Phi_f$ and rates of fluorescence are calculated from $k_f = 1/\tau_f = k_f^r + k^{nr} \cdot k^{nr}$ which indicates the rates of non-radiative decay. The rates of radiative fluorescence are found from $k_f^r = 1/\tau_0$. The radiative lifetimes, τ_0, are calculated by the formula [42,43]: $\tau_0 = 3.5 \times 10^8/(\nu_{max}^2 \times \varepsilon_{max} \times \Delta\nu_{1/2})$, where ν_{max} is the wavenumber per centimeter, ε_{max} is the molar extinction coefficient at the selected absorbance wavelength, and $\Delta\nu_{1/2}$ is the half-width of the selected absorbance in wavenumber unit. Photophysical properties of the studied compounds in solvents of different polarity are given in Table 2. In general, it is seen that higher the polarity of the solvents, higher the calculated fluorescence lifetimes of the compounds. The higher lifetime in chloroform compared to the other solvents supports the intermolecular hydrogen bonding enolic form of thienylidene azo dyes **4a–b** in excited state. However, both the lowest τ_f value and the smallest Stokes shift in ethyl acetate indicate the low probability of tautomerization. In general, k_f^r and k^{nr} values decrease with increasing polarity. Lower non-radiative decay constant value ($3.7 \times 10^9\ s^{-1}$) for compound **4a** in chloroform with respect to corresponding values in other solvents indicates the

Table 2
Fluorescence emission data, fluorescence quantum yields (Φ_F), radiative lifetimes (τ_0/ns), fluorescence lifetimes (τ_f/ns), fluorescence rate constants ($k_f^r \times 10^7/s^{-1}$), non-radiative rate constants ($k^{nr} \times 10^9/s^{-1}$), and singlet energies (E_s/(kcal/mol)) of thienylidene azo dyes **4a–b** in solvents of different polarity ($\lambda_{exc} = 480$ nm)

Solvent	Compound	Φ_f	τ_0	τ_f	k_f^r	k^{nr}	E_s
Toluene	**4a**	0.0040	25.4	0.10	3.9	10.0	59.6
	4b	0.0046	8.2	0.04	12.1	24.9	59.2
Chloroform	**4a**	0.0095	28.0	0.27	3.6	3.7	58.5
	4b	0.0060	11.5	0.07	8.7	14.2	58.0
Ethyl acetate	**4a**	0.0040	15.7	0.06	6.4	16.6	60.4
	4b	0.0035	13.3	0.05	7.5	19.9	59.7
Tetrahydrofuran	**4a**	0.0087	23.7	0.20	4.2	4.9	59.6
	4b	0.0038	19.4	0.07	5.1	14.2	58.6
Dichloromethane	**4a**	0.0057	43.0	0.24	2.3	4.1	57.8
	4b	0.0036	21.0	0.08	4.8	12.5	57.4

inhibition of fluorescence quenching and supports the more planar structure of compound **4a** in chloroform.

3.2. Thermal degradation and photoirradiation studies

Thermal stabilities of the synthesized compounds have been tested by thermogravimetric analysis under nitrogen atmosphere as shown in TGA curves in Fig. 5. Della-Casa et al. have compared the thermogravimetric analysis of a series of copolymer consisting of azobenzene-substituted thiophenes and found that the first weight loss from the compounds starts 338 °C and the second one starts at 480 °C [44]. Mohamed et al. have reported the thermal behavior of a schiff base derived from 2-thiophenecarboxaldehyde and 2-aminobenzoic acid and found that derivative TG curves of the compound show peaks at 260 °C and 470 °C [45]. The derivative TG curves of azo dyes **1a** and **1b** exhibit degradation peaks centered at about 306 °C and 308 °C, respectively. The derivative TG curves show two degradation peaks, one centered at about 270 °C and the other centered at about 438 °C for azo dye **2a**. For azo dye **2b**, two degradation peaks are observed at about 269 °C for the first loss range and at about 446 °C for the second.

The TGA curves for thienylidene azo dyes **4a–b** show that the weight losses begin at about 150 °C for both the compounds. The derivative TG curves for thienylidene azo dye **4a** exhibit degradation peaks centered at about 220 °C, 262 °C, and 476 °C. The TGA curve for thienylidene azo dye **4a** refers to three stages of mass losses within the temperature range 50–990 °C. The first stage at 150–340 °C with a mass loss of 47.1% (calcd. 46.4%) corresponds to the loss of $C_{11}H_7N_2O_2S$. The second stage at 340–520 °C with a mass loss of 23.6% (calcd. 24.1%) corresponds to the loss of $C_6H_4N_2O$, and the compound **4a** loses 12.5% of its weight at the last stage within the temperature range 520–990 °C. Also, thienylidene azo dye **4b** shows similar degradation behavior and gives three stages of mass losses at the same temperature scale. The first stage at 150–325 °C with a mass loss of 52.6% (calcd. 52.5%) corresponds to the loss of $C_{11}H_6N_3O_2SCl$. The second stage of decomposition at the temperature range 325–550 °C is roughly assigned to the loss of C_6H_4O with a mass loss 15.3% (calcd. 17.2%). Thus, 15.1% of its weight is loosed within the temperature range 550–990 °C at the last stage.

Photoisomerization behavior of azobenzene chromophores between *trans*-isomer and *cis*-isomer upon light irradiation has been well discussed in literatures [13,46–48]. It is well-known that the more stable *trans*-isomer can be converted to the less stable *cis*-isomer by UV light irradiation exciting the $\pi-\pi^*$ electronic transition, and reverse change can be carried out by visible light irradiation exciting the $n-\pi^*$ electronic transition or by heating. In our studies, photoisomerization of thienylidene azo dyes **4a–b** as indicated in Scheme 3 has been followed by monitoring the decrease or increase in their fluorescence intensity upon Xe light irradiation for 1 h. −N=N− bonds of the compounds have been excited with UV light at 254 nm for obtaining the *cis*-isomer, and the *cis*-to-*trans* photoisomerization has been driven by exciting the sample with visible light at 480 nm. The data are acquired at the emission wavelength of 530 nm. All measurements are performed in ethyl acetate.

While emission intensity resulted from the excitation with UV light at the wavelength of 254 nm slightly decreases or remains stable, the corresponding spectra obtained from the excitation with visible light at 480 nm significantly increase as shown in Fig. 6a. Photoisomerization of the compounds is evaluated by the calculation of rate constants. According to the fittings as shown in Fig. 6b, photoisomerization rate constants of the compounds are calculated with the formula, $\ln(I_0/I) = k_{c\text{-}t} \times t$ where I_0 and I are the emission intensities of the compound before and after the irradiation, respectively, $k_{c\text{-}t}$ is the rate constant of *cis*-to-*trans* isomerization, and t is the irradiation time. Tawa et al. have reported that the $k_{c\text{-}t}$ values for the azo dyes covalently bonded to the styrene copolymer have been found to be $8 \times 10^{-6}\ s^{-1}$ [46]. The *cis*-to-*trans* photoisomerization rate constants of compounds **4a** and **4b** have been found to be about 4.7×10^{-5}, and $6.3 \times 10^{-5}\ s^{-1}$, respectively. These values are 6–7 times higher than the *trans*-to-*cis* photoisomerization rate constants obtained by the UV excitation experiments at 254 nm. Increment in emission intensity in *trans* form may indicate that the more planar form of the compound is formed and

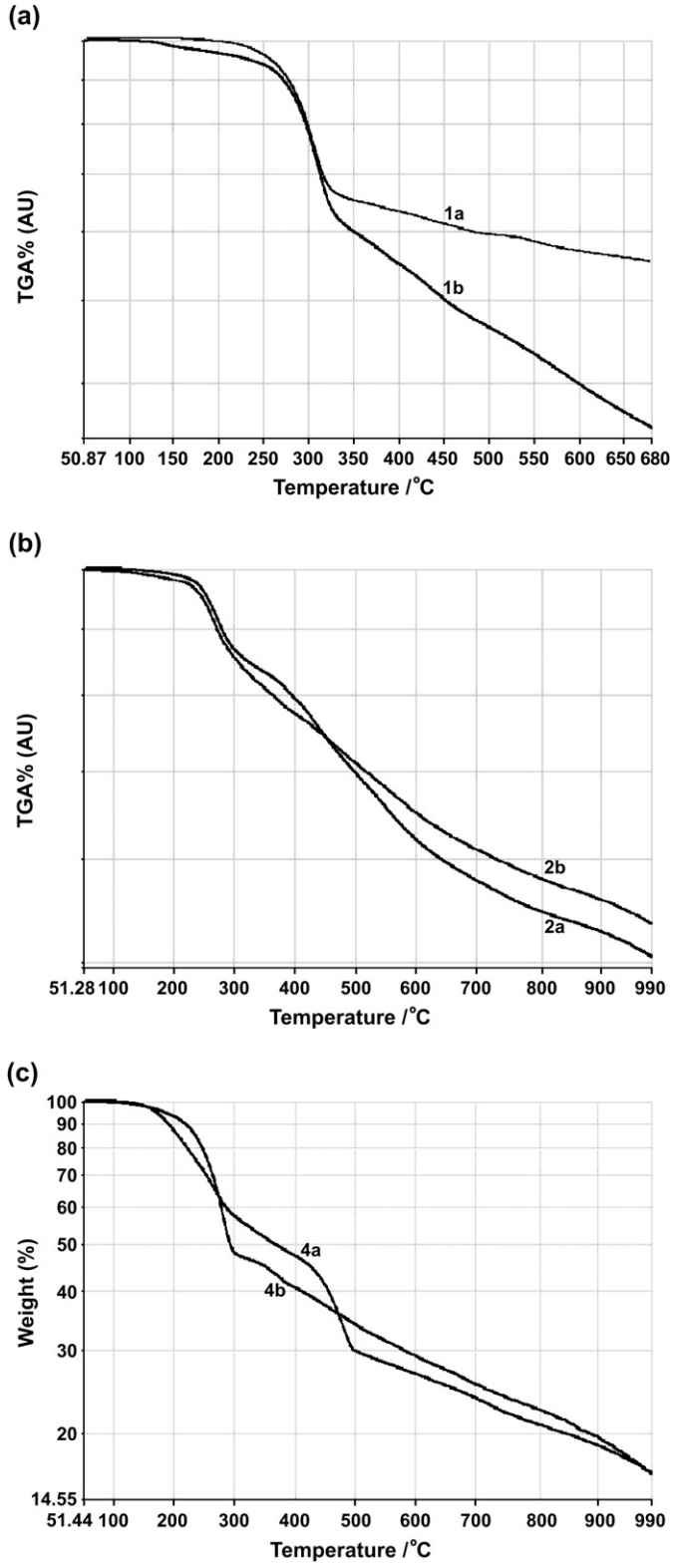

Fig. 5. TGA curves of (a) azo dyes **1a–b**, (b) azo dyes **2a–b**, and (c) thienylidene azo dyes **4a–b**.

fluorescence quenching probability is reduced inside the molecule. In *cis* form, bulky aromatic structures containing strong electron acceptor ($-NO_2$) and electron donor ($-N(CH_3)_2$) groups come close to each other so that fluorescence

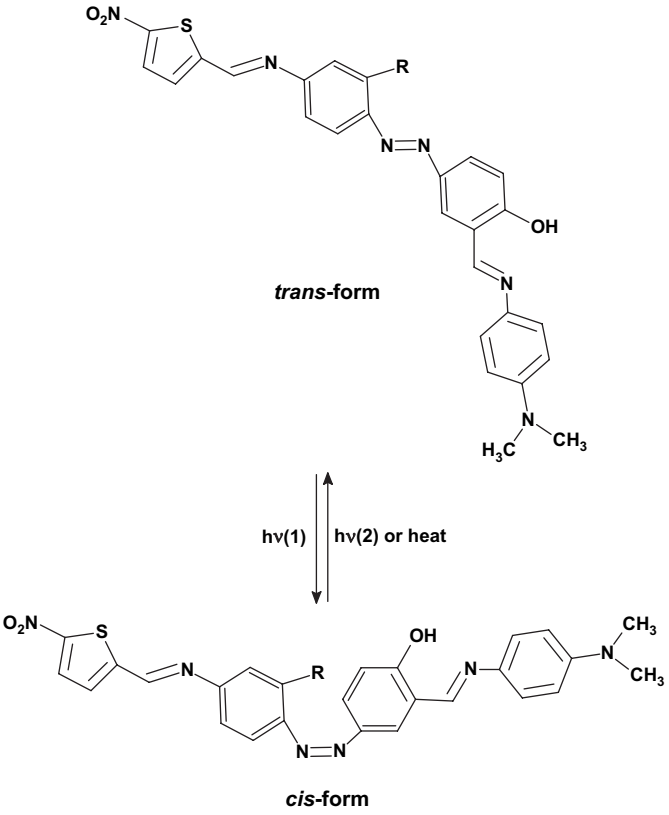

Scheme 3. Photoisomerization of thienylidene azo dyes **4a–b**.

quenching or electron transfer process may be occur. Therefore, fluorescence quantum yield of the compounds in *trans* form is higher than that in *cis* form.

3.3. CV measurements and fluorescence quenching experiments

There have been a variety of articles on the spectroelectrochemical behaviors of azobenzene functionalities in literatures [13,18,20,27,49]. One of which was prepared by Khandar and Nejati. They have studied the electrochemical properties of a series of copper (II) complexes with azo-linked salicylaldimine Schiff base ligands. Cyclic voltammetry indicates that compounds have quasi-reversible redox behavior and some of the complexes give irreversible and reversible reduction [18]. The redox potentials of thienylidene azo dyes **4a–b** are measured by the use of cyclic voltammetry in [TBA][PF6]–acetonitrile solution. The cyclic and differential pulse voltammograms of the compounds are illustrated in Figs. 7 and 8, and the corresponding characteristic data are summarized in Table 3. The cyclic voltammogram of compound **4a** exhibits three reversible reduction waves, the first of which is observed at −0.58 V, second of which is at −0.75 V, and the smallest value is obtained at −1.28 V. Also, two irreversible oxidation waves are observed for compound **4a** at 0.87 V and at 1.25 V. The cyclic voltammetry of compound **4b** shows two reversible waves, one of which is appeared at −0.78 V, and the other is observed at −1.28 V. Also, a reversible oxidation wave is

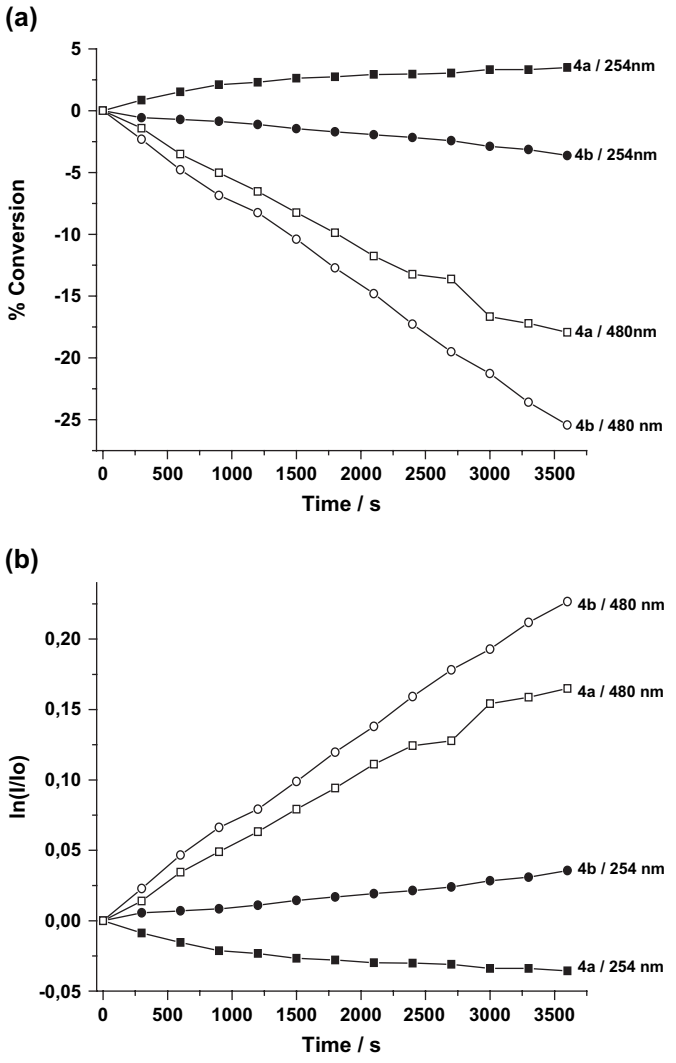

Fig. 6. (a) Conversion (%) of thienylidene azo dyes **4a–b** under Xe lamp exposure in the fluorescence spectrophotometer in ethyl acetate at the excitation wavelength of 254 nm or 480 nm for 1 h ($\lambda_{em} = 530$ nm), and (b) the corresponding Stern–Volmer plots (for **4a**/254 nm: $8.4 \times 10^{-6}X - 0.00929$; R^2: 0.92, for **4a**/480 nm: $4.7 \times 10^{-5}X + 0.00527$; R^2: 0.99, for **4b**/254 nm: $9.1 \times 10^{-6}X + 0.00074$; R^2: 0.99, and for **4b**/480 nm: $6.3 \times 10^{-5}X + 0.00561$; R^2: 0.99).

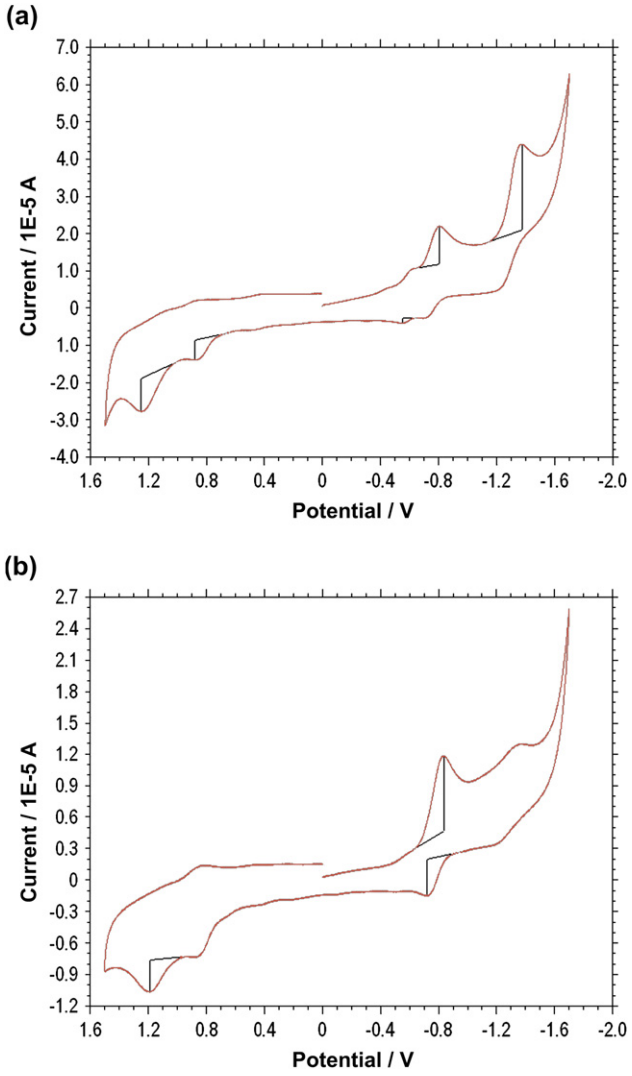

Fig. 7. Cyclic voltammograms of (a) thienylidene azo dye **4a**, and (b) thienylidene azo dye **4b** in acetonitrile containing 100 mM [TBA][PF6].

observed at 0.85 V and an irreversible wave is observed at 1.20 V for compound **4b**. Differential pulse voltammograms of the studied compounds illustrated in Fig. 8a and b confirm the formation of reduction waves at the indicated values. Decrease in oxidation potential evaluated above suggests that electron-withdrawing capacity of compound **4b** is greater than that of compound **4a** because of the electron acceptor behavior of chloride atom through sigma bond.

The LUMO energy level of the compounds are calculated by the formula: $E_{LUMO} = -\left(4.8 + E^{red}_{onset}\right)$ eV, where E^{red}_{onset} indicates the onset value of reduction potential. Reference energy value of ferrocene below the vacuum level is taken as −4.8 eV [50]. The LUMO energy levels of the compounds are found to be −3.07 eV. In addition, HOMO energy levels of the compounds have been determined by subtracting the band gap energies obtained from the onset of the visible absorption spectra from the LUMO level. The energy gap values read on CV graph are well correlated with calculated values from the visible absorption spectra. The HOMO energy levels of the compounds **4a** and **4b** are found to be −5.61 eV and −5.59 eV, respectively. Band gap values are 2.54 eV and 2.52 eV for **4a** and **4b**, respectively. Molecular structures of compounds **4a** and **4b** with LUMO energy levels lower than that of TiO_2 conduction band may be used as hole conducting materials in solid DSSC (Dye Sensitized Solar Cell) devices.

To better understand the photosensitized interaction mechanisms and to evaluate the electron donor/acceptor ability towards the different quenchers, fluorescence quenching experiments of thienylidene azo dyes **4a–b** with electron acceptor (Co^{2+}) and electron donors (anthracene, pyrene) have been carried out. The solution of 8.6×10^{-2} M Co $(NO_3)_2 \cdot 6H_2O$ was prepared in THF and at each addition 20 μl of this solution was poured into the 3 ml THF solution of 3×10^{-5} M compounds **4a–b** which were placed in a quartz cuvette. After each addition, decline in fluorescence intensity of compounds **4a–b** was followed and no new emission

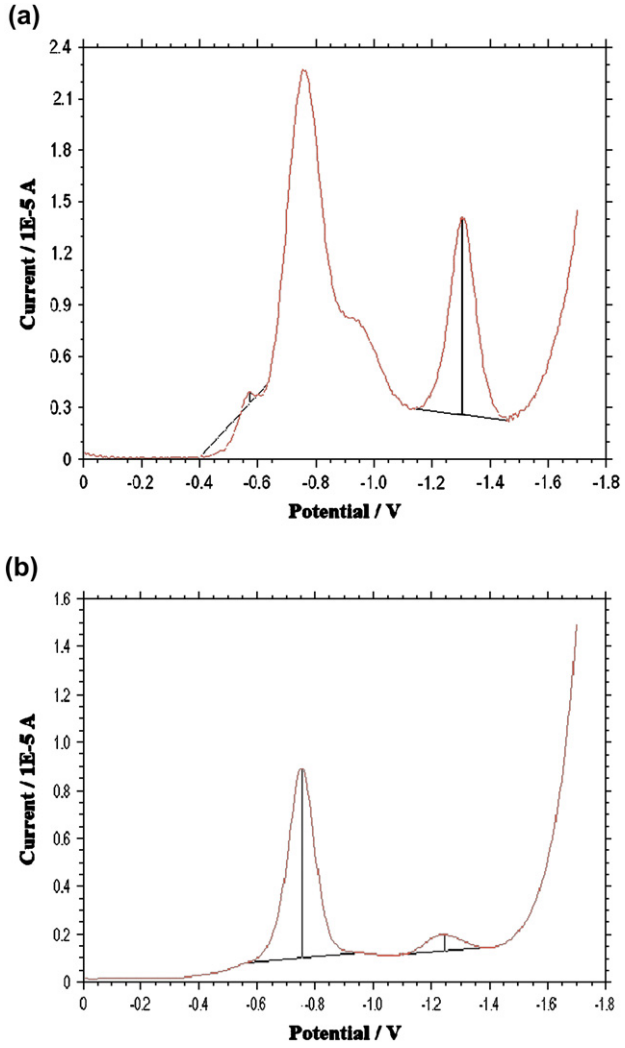

Fig. 8. Differential pulse voltammograms of (a) thienylidene azo dye **4a**, and (b) thienylidene azo dye **4b** in acetonitrile containing 100 mM [TBA][PF6].

band was observed (Fig. 9a). Electron acceptor capacities of the compounds towards the π-electron rich aromatics of anthracene and pyrene were examined with the same procedure. The solutions of anthracene and pyrene in THF were at the concentrations of 1×10^{-6} M. As shown in Fig. 10a, decline in fluorescence intensities of these donor molecules is detected with the increasing concentrations of compounds **4a** and **4b** in THF solution prepared at initial concentrations of 5.9×10^{-4} M and 3.3×10^{-4} M, respectively. Any detectable wavelength shift of donor emission is obtained. The fluorescence intensities at various concentrations are fit to the Stern–Volmer relationship given below [51].

$$I_0/I = 1 + k_q \tau_0 [Q],$$

where I_0 and I are the fluorescence intensities in the absence and presence of quenchers, respectively, and k_q is the bimolecular electron transfer rate constant, and τ_0 is the radiative lifetime in the absence of the quencher. Radiative lifetime values of pyrene and anthracene are taken as 322 ns and 5.3 ns, respectively [30]. Corresponding Stern–Volmer plots are shown in Figs. 9b and 10b.

Rate constant of fluorescence quenching between compound **4a** and strong electron acceptor Co^{2+} ions is equal to the value of $2.1 \times 10^{14}\ M^{-1}\ s^{-1}$ as given in Table 4. Co^{2+} ions may interact with the nitrogen atom of the Schiff base and the polar oxygen atom of the hydroxyl group attached to the salicylaldimine ligand and take place in this position of the ring system. For this reason, quenching value is quite high for compounds **4a–b**. Fluorescence quenching rate constant between strong electron donor pyrene and compound **4b** is approximately 2-fold of the corresponding value between pyrene and compound **4a**. Also, k_q value for anthracene-compound **4b** quenching is approximately 1.4 times greater than that of anthracene-compound **4a** quenching. One may infer from these results that compound **4b** is more electron-withdrawing character with relative to compound **4a** towards the condensed aromatic rings of pyrene and anthracene. All of the calculated k_q values are above the diffusion rate limits of $1 \times 10^{10}\ M^{-1}\ s^{-1}$. These high quenching rates may be taken as evidences of occurrence of photo-electron transfer process and formation of contact radical ion pairs in the excited state. In THF solution, the planarity of the system resulted from the possibility of intermolecular hydrogen bonding enolic form of thienylidene azo dyes **4a–b** may have caused the favorable donor/acceptor interaction. Also, electron acceptor behavior of azo chromophore and strong electron-withdrawing capacity of nitro group attached to thiophene ring may facilitate the formation of radical anion structure.

Quenching data can be analyzed by using the formula as given below [52]

$$\Delta G_{ET} = 23.06\left[E\left(D^+/D\right) - E\left(A/A^-\right)\right] - E^*_D$$

ΔG_{ET} (kcal/mol), free energy of electron transfer, can be determined from the oxidation potential of the donor, the reduction potential of the acceptor, and the excited state energy of the sensitizer. The free energies of photo-electron transfer process (ΔG_{ET}) between the azo dyes and the quenchers are found to be about −19 kcal/mol. All of the calculated free energy changes are below the value of −5 kcal/mol (the ''rule of thumb'') [53]. These data can be taken as proofs that photo-electron transfer process occurs between the quenchers and sensitizer molecules and contact radical ion pairs are generated.

Table 3
Cyclic voltammetry data for thienylidene azo dyes **4a– b**

Dye	E_{red} (V)	E_{ox} (V)	E^{red}_{onset} (V)	E_g (eV)	HOMO (eV)	LUMO (eV)
4a	−0.58, −0.75, −1.28	0.87, 1.25	−1.73	2.54 (2.53)	−5.61	−3.07
4b	−0.78, −1.28	0.85, 1.20	−1.73	2.52 (2.48)	−5.59	−3.07

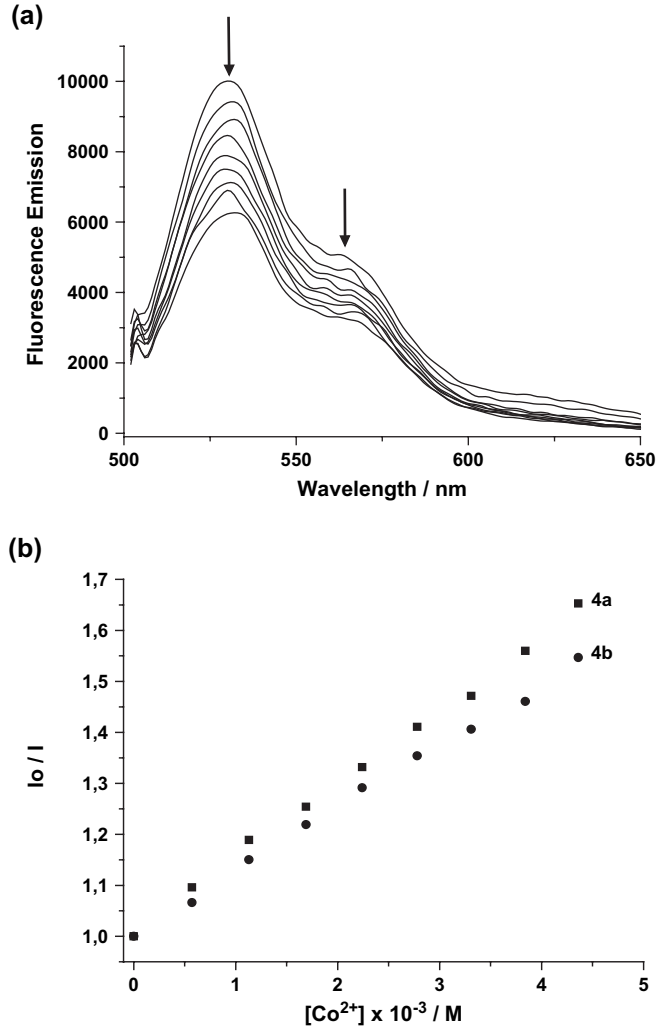

Fig. 9. (a) Fluorescence emission quenching of thienylidene azo dye **4a** with increasing Co^{2+} concentration in tetrahydrofuran solution ($\lambda_{exc} = 480$ nm), and (b) the corresponding Stern–Volmer plots (for **4a**: $144.47X + 1.00982$; R^2: 0.99, for **4b**: $122.91X + 1.00516$; R^2: 0.99).

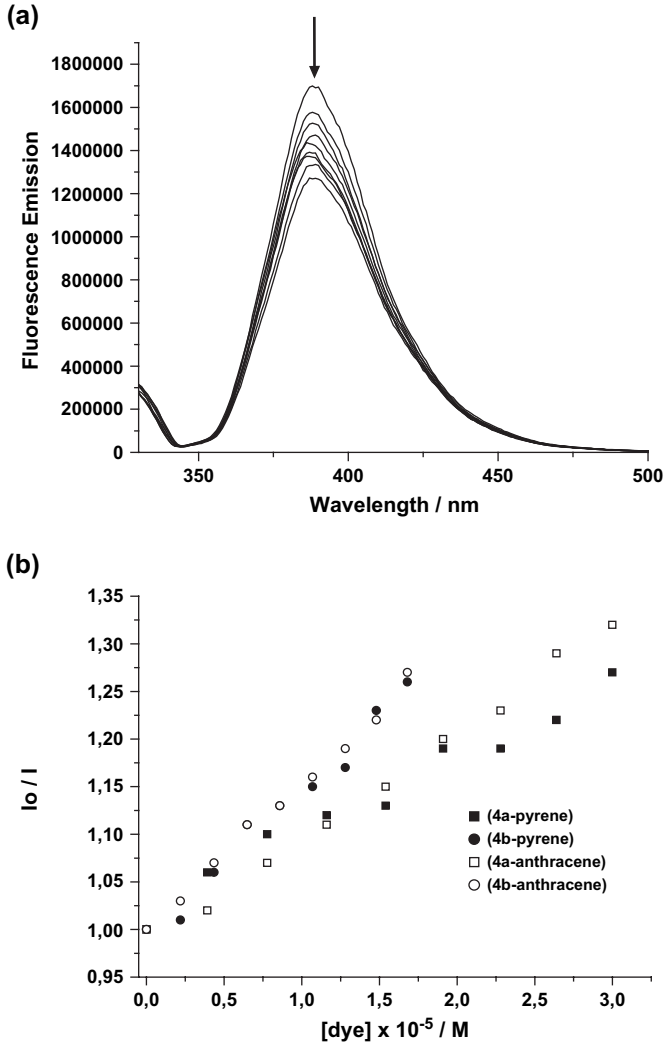

Fig. 10. (a) Fluorescence emission quenching of pyrene with increasing thienylidene azo dye **4a** concentration in tetrahydrofuran solution ($\lambda_{exc} = 320$ nm), and (b) the corresponding Stern–Volmer plots (for **4a**-pyrene: $0.08049X + 1.0197$; R^2: 0.98, for **4b**-pyrene: $0.15528X + 0.9921$; R^2: 0.99, $\lambda_{exc}^{anth} = 340$ nm, for **4a**-anthracene: $0.11105X + 0.9854$; R^2: 0.99, for **4b**-anthracene: $0.15373X + 1.00008$; R^2: 0.99).

3.4. Changes in absorption spectra of the complexes with copper(II) ions

The complexation processes of thienylidene azo dyes **4a–b** with copper(II) ions were studied in MeCN solution. At each addition 40 μl of $CuCl_2$ solution prepared in MeCN at the concentration of 5×10^{-4} M was poured into the 3 ml MeCN solution of 1.2×10^{-4} M compounds **4a–b**. After each addition, changes in absorbances of compounds **4a–b** were monitored and new absorption bands were observed (Fig. 11). The absorption spectra of copper(II) complexes of thienylidene azo dyes **4a–b** give blue shifts at n–π* transition in the visible region as compared to the visible absorption spectra of uncomplexed form of the dyes. More gradual blue shifts from 377 nm to 356 nm for compound **4a** and from 343 nm to 318 nm for compound **4b** are observed in presence of copper(II) ions. Also, new UV absorption peaks are observed at the wavelength of 255 nm for both the compounds. Copper(II) alone gives absorption peaks at the wavelengths of 462 nm, 310 nm, and 260 nm (data not shown).

Copper(II) ion is mainly complexed with the non-bonding electron pair of the oxygen atom belonging to the hydroxyl group and the nitrogen atom of the imine group. Also, energy increase of the intense π–π* transition of compounds at wavelength of 300–380 nm is due to the complexation

Table 4
Fluorescence quenching rate constants ($k_q/M^{-1}\,s^{-1}$) calculated from the Stern–Volmer plots of the corresponding quenchers and Gibbs free energies (ΔG_{ET}/(kcal/mol)) of the acceptor (Co^{2+}) and donor (pyrene and anthracene) molecules

Compound	Quenchers	k_q	ΔG_{ET}
4a	Co^{2+}	2.1×10^{14}	−19.7
Pyrene	**4a**	2.5×10^{11}	−19.2
Anthracene	**4a**	2.1×10^{13}	−19.9
4b	Co^{2+}	4.5×10^{14}	−18.7
Pyrene	**4b**	4.8×10^{11}	−19.2
Anthracene	**4b**	2.9×10^{13}	−19.9

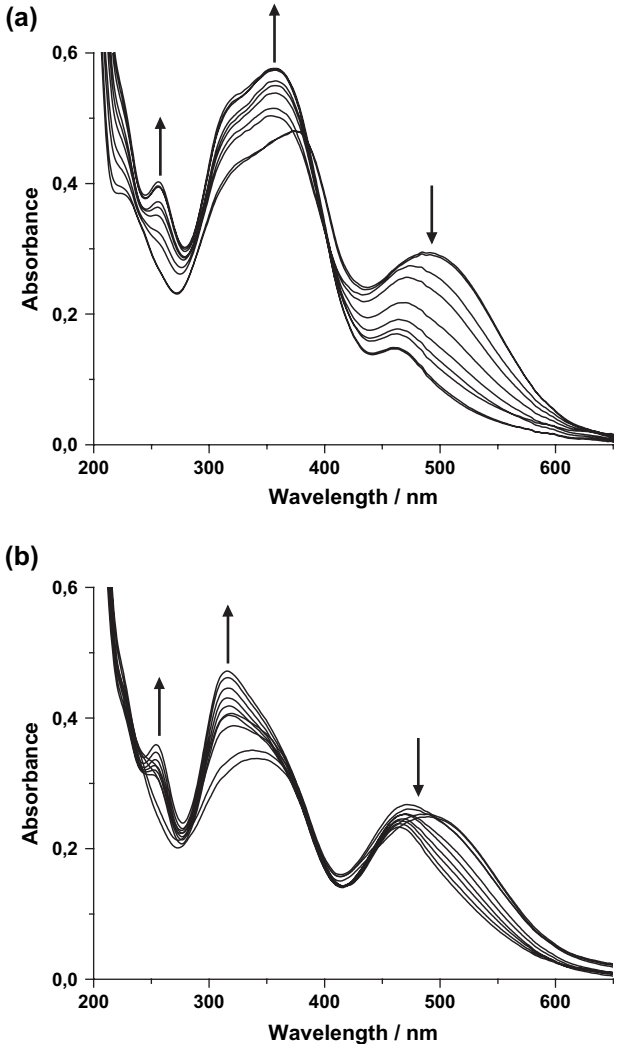

Fig. 11. Changes in UV–vis absorption spectra of (a) thienylidene azo dye **4a** (1.2×10^{-4} mol l^{-1}), and (b) thienylidene azo dye **4b** (1.2×10^{-4} mol l^{-1}) by adding Cu^{2+} ions in MeCN during the complex formation. Arrows indicate a change in the absorbance with increase in the concentration of Cu^{2+} (mol l^{-1}): From down to up 0, 6.6×10^{-6}, 1.3×10^{-5}, 1.9×10^{-5}, 2.5×10^{-5}, 3.1×10^{-5}, 3.7×10^{-5}, 4.3×10^{-5}, 4.8×10^{-5}, and 5.3×10^{-5}.

between copper(II) ion and azo ligand or imine group. A strong hyperchromic shift is observed for this region, while complexation of the dyes with the metal ion is responsible for a significant hypochromic shift at n–π* transition region.

4. Conclusions

In this study, new kind of azo dyes combining with salicyaldimine-based ligand and nitro-substituted thiophene moiety have been synthesized. The experimental results obtained in solvents of different polarity have revealed that increasing solvent polarity diminishes the LUMO energy level of the studied compounds with a higher ratio relative to the HOMO energy level, excluding in chloroform solution. Hydrogen bonding ability of the chloroform with the hydroxyl group facilitates formation of keto form of the compound. Long-wavelength emissions of the compounds indicate the keto structure.

Also, strong electron donor (alkylamino-) and strong electron acceptor (nitro-) group in the side chain of the compounds give a hyperpolarizability activity to the structure. Studied compounds behave as an electron acceptor towards π-electron rich aromatics of pyrene and anthracene because of the electron-withdrawing capacity of azo group, but behave as an electron donor towards acceptor Co^{2+} ions. Chelating of thienylidene azo dyes **4a–b** with copper(II) ions have suggested that these compounds are also used as reagent for spectroscopic determination of trace amounts of Cu^{2+} with the detection limit of between 6.6×10^{-6} and 5.3×10^{-5} mol l^{-1}.

Acknowledgements

The authors would like to thank the Research Council of Celal Bayar University (BAP), Alexander von Humboldt Foundation (AvH) and the State Planning Organization of Turkey (DPT) for the financial support of this research, and Özgül Haklı for carrying out mass spectrometry analysis of the azo dyes **2a–b**.

References

[1] Ho MS, Barrett C, Paterson J, Esteghamatian M, Natansohn A, Rochon P. Synthesis and optical properties of poly{(4-nitrophenyl)-[3-[*N*-[2-(methacryloyloxy)ethyl]-carbazolyl]]diazene}. Macromolecules 1996;29:4613–8.

[2] Boogers JOF, Klaase PTA, De Vlieger JJ, Alkema DPW, Tinnemans AHA. Cross-linked polymer materials for nonlinear optics. 1. UV-cured acrylic monomers bearing azobenzene dyes. Macromolecules 1994;27:197–204.

[3] Yin S, Xu H, Shi W, Gao Y, Song Y, Wing J, et al. Synthesis and optical properties of polyacetylenes containing nonlinear optical chromophores. Polymer 2005;46:7670–7.

[4] Ho MS, Natansohn A. Azo polymers for reversible optical storage. 7. The effect of the size of the photochromic groups. Macromolecules 1995;28:6124–7.

[5] Nabeshima Y, Shishido A, Kanazawa A, Shiono T, Ikeda T, Hiyama T. Synthesis of novel liquid-crystalline thiophene derivatives and evaluation of their photo responsive behavior. Chem Mater 1997;9:1480–7.

[6] Hallas G, Towns AD. Dyes derived from aminothiophenes. Part 4: synthesis of some nitro-substituted thiophene-based azo disperse dyes. Dyes Pigments 1997;33(4):319–36.

[7] Hallas G, Towns AD. Dyes derived from aminothiophenes. Part 7: synthesis and properties of some benzo[*b*]thiophene-based azo disperse dyes. Dyes Pigments 1997;35(3):219–37.

[8] Towns AD. Developments in azo disperse dyes derived from heterocyclic diazo components. Dyes Pigments 1999;42:3–28.

[9] Isak SJ, Eyring EM, Spikes JD, Meekins PA. Direct blue dye solutions: photo properties. J Photochem Photobiol A 2000;134:77–85.

[10] Guo S, Li D, Zhang W, Pu M, Evans DG, Duan X. Preparation of an anionic azo pigment-pillared layered double hydroxide and the thermo- and photostability of the resulting intercalated material. J Solid State Chem 2004;177:4597–604.

[11] Vig A, Sirbiladze K, Nagy HJ, Aranyosi P, Rusznák I, Sallay P. The light stability of azo dyes and dyeings V. The impact of the atmosphere on the light stability of dyeings with heterobifunctional reactive azo dyes. Dyes Pigments 2006;71:199–205.

[12] Raposo MMM, Sousa AMRC, Fonseca AMC, Kirsch G. Thienylpyrrole azo dyes: synthesis, solvatochromic and electrochemical properties. Tetrahedron 2005;61:8249–56.

[13] Kurihara M, Nishihara M. Azo- and quinone-conjugated redox complexes—photo- and proton-coupled intramolecular reactions based on d–π interaction. Coord Chem Rev 2002;226:125–35.
[14] Hoshino N, Murakami H, Matsunaga Y, Inabe T, Maruyama Y. Liquid crystalline copper(II) complexes of *N*-salicylideneaniline derivatives. Mesomorphic properties and a crystal structure. Inorg Chem 1990;29: 1177–81.
[15] Baena MJ, Barberá J, Espinet P, Ezcurra A, Ros MH, Serrano JL. Ferroelectric behavior in metal-containing liquid crystals: a structure–activity study. J Am Chem Soc 1994;116:1899–906.
[16] Gegiou D, Lambi E, Hadjoudis E. Solvatochromism in *N*-(2-hydroxy benzylidene)aniline, *N*-(2-hydroxybenzylidene)benzylamine, and *N*-(2-hydroxybenzylidene)-2-phenylethylamine. J Phys Chem 1996;100: 17762–5.
[17] Taşcıoğlu S, Yalçın B, Nasrullayeva TM, Andaç Ö, Büyükgüngör O, Aydın A, et al. The syntheses, structure and properties of cobalt complexes with β-alanine derivatives. Polyhedron 2006;25:1279–86.
[18] Khandar AA, Nejati K. Synthesis and characterization of a series of copper(II) complexes with azo-linked salicylaldimine schiff base ligands. Crystal structure of Cu5PHAZOSALTN.$CHCl_3$. Polyhedron 2000;19: 607–13.
[19] Khandar AA, Rezvani Z. Preparation and thermal properties of the bis[5-((4-heptyloxyphenyl)azo)-*N*-(4-alkoxyphenyl)-salicylaldiminato]copper(II) complex homologues. Polyhedron 1999;18:129–33.
[20] Reddinger JL, Reynolds JR. Tunable redox and optical properties using transition metal-complexed polythiophenes. Macromolecules 1997;30: 673–5.
[21] Angelino MD, Laibinis PE. Synthesis and characterization of a polymer-supported salen ligand for enantioselective epoxidation. Macromolecules 1998;31:7581–7.
[22] Kaya I, Yıldız M, Koyuncu M. The synthesis and characterization of new oligo(polyether)s with schiff base type. Synth Met 2002;128:267–72.
[23] Kaya I, Koyuncu S. The synthesis and characterization of oligo-*N*-4-aminopyridine, oligo-2-[(pyridine-4-yl-imino) methyl] phenol and its some oligomer–metal complexes. Polymer 2003;44:7299–309.
[24] Cazacu M, Marcu M, Vlad A, Rusu GI, Avadanei M. Chelate polymers. VI. New copolymers of the some siloxane containing bis(2,4-dihy droxybenzaldehyd-imine)Me^{2+} with bis(*p*-carboxyphenyl)diphenylsilane. J Organomet Chem 2004;689:3005–11.
[25] Kaya I. Synthesis, characterization and optimum reaction conditions of oligo-*N*,*N*′-bis (2-hydroxy-1-naphthalidene) thiosemicarbazone. J Polym Res 2004;11:175–80.
[26] Kaya I, Gül M. Synthesis, characterization and thermal degradation of oligo-2-[(4-fluorophenyl) iminomethylene] phenol and some of its oligomer–metal complexes. Eur Polym J 2004;40:2025–32.
[27] Zagórska M, Kulszewicz-Bajer I, Pron A, Sukiennik J, Raimond P, Kajzar F, et al. Preparation and spectroscopic and spectroelectrochemical characterization of copolymers of 3-alkylthiophenes and thiophene functionalized with an azo chromophore. Macromolecules 1998;31:9146–53.
[28] Morley JO, Naji M, Hutchings MG, Hall N. Resonance-enhanced optical nonlinearities in azothiophenes. J Phys Chem A 1998;102:5802–8.
[29] Kubin RF, Fletcher AN. Fluorescence quantum yields of some rhodamine dyes. J Lumin 1982;27:455–62.
[30] Scannell MP, Fenick DJ, Yeh SR, Falvey DE. Model studies of DNA photorepair: reduction potentials of thymine and cytosine cyclobutane dimers measured by fluorescence quenching. J Am Chem Soc 1997;119:1971–7.
[31] Skoog DA, Leary JJ. Principles of instrumental analysis. 4th ed. Philedelphia: Saunders; 1992.
[32] Scoog DA, West DM, Holler FJ. Fundamentals of analytical chemistry. 7th ed. London: Saunders; 1996.
[33] Botros R. Azomethine dyes derived from an *o*-hydroxy aromatic aldehyde and a 2-aminopyridine. US Patent 4,051,119; 1977.
[34] Bellamy FD, Qu K. Selective reduction of aromatic nitro compounds with stannous chloride in non acidic and non aqueous medium. Tetrahedron Lett 1984;25(8):839–42.
[35] Guha D, Mandal A, Koll A, Filarowski A, Mukherjee S. Proton transfer reaction of a new *ortho*hydroxy schiff base in protic solvents at room temperature. Spectrochim Acta Part A 2000;56:2669–77.
[36] Ogawa K, Harada J, Fujiwara T, Yoshida S. Thermochromism of salicylideneanilines in solution: aggregation-controlled proton tautomerization. J Phys Chem A 2001;105:3425–7.
[37] Koll A, Filarowski A, Fitzmaurice D, Waghorne E, Mandal A, Mukherjee S. Excited state proton transfer reaction of two new intramolecularly hydrogen bonded schiff bases at room temperature and 77 K. Spectrochim Acta Part A 2002;58:197–207.
[38] Mukhopadhyay M, Banerjee D, Koll A, Filarowski A, Mukherjee S. Proton transfer reaction of a new orthohydroxy schiff base in some protic and aprotic solvents at room temperature and 77 K. Spectrochim Acta Part A 2005;62:126–31.
[39] Alarcón SH, Pagani D, Bacigalupo J, Olivieri AC. Spectroscopic and semi-empirical MO study of substituent effects on the intramolecular proton transfer in anils of 2-hydroxybenzaldehydes. J Mol Struct 1999;475:233–40.
[40] Scaiano JC. CRC handbook of organic photochemistry, vol. II. Florida: CRC Press Inc.; 1989.
[41] Joshi H, Kamounah FS, Gooijer C, van der Zwan G, Antonov L. Excited state intramolecular proton transfer in some tautomeric azo dyes and schiff bases containing an intramolecular hydrogen bond. J Photochem Photobiol A 2002;152:183–91.
[42] Suppan P. Chemistry and light. London: The Royal Society of Chemistry; 1994.
[43] Turro NJ. Molecular photochemistry. London: Benjamin; 1965.
[44] Della-Casa C, Fraleoni-Morgera A, Lanzi M, Costa-Bizzarri P, Paganin L, Bertinelli F, et al. Preparation and characterization of thiophene copolymers with second order non-linear optical properties. Eur Polym J 2005;41:2360–9.
[45] Mohamed GG, Omar MM, Hindy AMM. Synthesis, characterization and biological activity of some transition metals with schiff base derived from 2-thiophene carboxaldehyde and aminobenzoic acid. Spectrochim Acta Part A 2005;62:1140–50.
[46] Tawa K, Zettsu N, Minematsu K, Ohta K, Namba A, Tran-Cong Q. Photoinduced reorientation of azo-dyes covalently linked to a styrene copolymer in bulk state. J Photochem Photobiol A 2001;143:31–8.
[47] Zhang Y, Lu Z, Deng X, Liu Y, Tan C, Zhao Y, et al. Photochromism and holographic recording in polymer film containing chiral azo molecules derived from amino acid. Opt Mater 2003;22:187–92.
[48] Mohr GJ, Grummt UW. Photochemistry of the amine-sensor dye 4-*N*,*N*-dioctylamino-4-trifluoroacetylazobenzene. J Photochem Photobiol A 2004;163:341–5.
[49] Kaim W, Doslik N, Frantz S, Sixt T, Wanner M, Baumann F, et al. Azo compounds as electron acceptor or radical ligands in transition metal species: spectroelectrochemistry and high-field EPR studies of ruthenium, rhodium and copper complexes of 2, 2′-azobis(5-chloropyrimidine). J Mol Struct 2003;656:183–94.
[50] Pommerehne J, Vestweber H, Guss W, Mahrt RF, Bassler H, Porsch M, et al. Efficient 2-layer LEDs on a polymer blend basis. Adv Mater 1995;7(6):551–4.
[51] Lakowicz JR. Principles of fluorescence spectroscopy, part 8. New York: Kluwer Academic/Plenum; 1999.
[52] Kavarnos GJ, Turro NJ. Photosensitization by reversible electron transfer: theories, experimental evidence, and examples. Chem Rev 1986;86:401–49.
[53] Jones G, Griffin SF, Choi CY, Bergmark WR. Electron donor–acceptor quenching and photoinduced electron transfer for coumarin dyes. J Org Chem 1984;49:2705–8.